The relative order of the p*M* values given in Table VI holds only for the conditions specified: 1 μM metal ion, 10 μM ligand, and p[H] 7.4. Under a different set of conditions the p*M* values would change and even the relative order could vary. As the value of p*M* increases so does the affinity of the ligand for the metal ion under the conditions specified. Table VI also provides a comparison of the distribution of metal ion between transferrin and both forms of EHPG for the trivalent metal ions Fe(III), Ga(III), and In(III). Since the stability constants for In(III)-transferrin complexes have not been measured, the correlation between log K_{ML} values for a series of ligands with Fe(III) and In(III) was used to arrive at a reasonable estimate of log K^*_{ML} and log $K^*_{M_2L}$ for In(III)-transferrin (Figure 11). The series of ligands chosen all contain phenolate (pyridinolate in the case of PLED), amino, and carboxylate donor groups analogous to those found in the active site of transferrin. The values of log K^*_{ML} and log $K^*_{M_2L}$ estimated for In(III)-transferrin are 18.8 and 17.9, respectively, at 25.0 °C, μ = 0.10 M, and $[HCO_3^-] = 1.4 \times 10^{-4}$ M. While the results in Table VI indicate that both EHPG complexes of Fe(III) and Ga(III) would be thermodynamically stable in the presence of transferrin, this is not the case for the In(III) complexes. Now whether these thermodynamically unfavorable reactions will also be sufficiently kinetically unfavorable to make the In-EHPG complexes less useful as radiopharmaceuticals will require additional kinetic studies.

Acknowledgment. This research was supported in part by Grant No. CA-42925 from the National Institutes of Health and by a grant from the Texas A&M Institute for Biosciences and Technology. C.J.B. wishes to thank the Robert A. Welch Foundation for a Predoctoral Fellowship. We also express our thanks to Ramunas Motekaitis for computational assistance.

Synthesis, Structure, and Bonding of Mononuclear Aryloxide Derivatives of Niobium in Oxidation States +5, +3, +2, and +1

Timothy W. Coffindaffer,[†] Bryan D. Steffy,[†] Ian P. Rothwell,*[,†,1] Kirsten Folting,[‡] John C. Huffman,[‡] and William E. Streib[‡]

Contribution from the Department of Chemistry, Purdue University, West Lafayette, Indiana 47907, and Molecular Structure Center, Indiana University, Bloomington, Indiana 47405. *Received August 5, 1988*

Abstract: The reduction of a series of niobium(V) aryloxides in the presence of the chelating phosphine dmpe (dmpe = $Me_2PCH_2CH_2PMe_2$) has been investigated. Treatment of hydrocarbon solutions of either $Nb_2(OAr\text{-}4Me)_{10}$ (**1a**) or $Nb_2(OAr\text{-}3,5Me_2)_{10}$ (**1b**) (OAr-4Me = 4-methylphenoxide; OAr-3,5Me_2 = 3,5-dimethylphenoxide) with sodium/amalgam (3 equiv) in the presence of dmpe (2 equiv) leads to the deep purple species $Nb(OAr\text{-}4Me)_2(dmpe)_2$ (**2a**) and $Nb(OAr\text{-}3,5Me_2)_2(dmpe)_2$ (**2b**), respectively. Spectroscopic and magnetic data on these compounds is consistent with them containing low spin d^3-configurations, while a solid-state structure of **2a** shows a pseudooctahedral environment about the niobium atom with mutually *trans*-aryloxide ligands. Treatment of **2b** with HOAr-3,5Me_2 (2 equiv) is found to lead to oxidation and the formation of a mixed-valence salt of composition $[Nb(OAr\text{-}3,5Me_2)_2(dmpe)_2]^+ [Nb(OAr\text{-}3,5Me_2)_6]^-$ (**3b**). Treatment of $Nb_2(OAr\text{-}3,5Me_2)_{10}$ with Na/Hg (1 equiv) in the presence of dmpe was also found to yield **3b**. The ^1H NMR of **3b** clearly show the noncontact shifted spectra for the low spin d^2-cation and d^0-anion. A solid-state study of **3b** confirmed the formulation and showed the monocation to contain *trans*-aryloxides as in the neutral **2a**. However, differences in the orientations of the aryloxide aryl rings within **2a** and **3b** were noted. The treatment of **2b** with CO (1 atm) was found to lead to the 18-electron dicarbonyl $Nb(OAr\text{-}3,5Me_2)(CO)_2(dmpe)_2$ (**4b**). A monocapped, trigonal-prismatic structure for **4b** was found in the solid state with the aryloxide ligand being the capping group. A small angle of only 66.7 (2)° was also found to exist between the two carbonyl groups in **4b**. The structural parameters in all of these molecules and in particular the Nb-OAr bond lengths and angles have been evaluated and discussed in terms of the importance of oxygen-p to metal-d π-bonding. In this context the solid-state (trigonal-bipyramidal) structure of the monomeric niobium(V) aryloxide $Nb(OAr\text{-}2,6Me_2)_5$ (**1c**) has also been determined for comparison. The summary of the crystal data is as follows: for $Nb(OAr\text{-}2,6Me_2)_5$ (**1c**) at 24 °C, a = 11.854 (6) Å, b = 16.305 (4) Å, c = 18.140 (5) Å, β = 99.44 (3)°, Z = 4, d_{calcd} = 1.312 g cm^{-3} in space group $P2_1/n$; for $Nb(OAr\text{-}4Me)_2(dmpe)_2$ (**2a**) at −158 °C, a = 12.646 (4) Å, b = 14.016 (5) Å, c = 9.707 (3) Å, α = 110.87 (2)°, β = 105.83 (2)°, γ = 76.21 (2)°, Z = 2, d_{calcd} = 1.321 g cm^{-3} in space group $P\bar{1}$; for $[Nb(OAr\text{-}3,5Me_2)_2(dmpe)_2][Nb(OAr\text{-}3,5Me_2)_6]$ (**3b**) at −156 °C, a = 27.96 (2) Å, b = 23.49 (2) Å, c = 13.32 (1) Å, β = 119.72 (3)°, Z = 4, d_{calcd} = 1.272 g cm^{-3} in space group $P2_1/a$; for $Nb(OAr\text{-}3,5Me_2)(CO)_2(dmpe)_2$ (**4b**) at −160 °C, a = 16.751 (3) Å, b = 12.133 (2) Å, c = 27.331 (7) Å, Z = 8, d_{calcd} = 1.364 g cm^{-3} in space group *Pcab*.

The last few years have seen a dramatic increase in research interest into the chemistry of the heavier group 5 elements (Nb, Ta) in their lower oxidation states. This interest has been prompted by the demonstrated high reactivity exhibited by low-valent niobium and tantalum complexes.[2-10] Activation of N_2, CO, acetylenes, and H_2 as well as the cleavage of CH bonds have all been associated with these types of complexes. Furthermore, the possibility for the formation of reactive metal-metal multiple bonds that are either novel or complimentary to their widely studied group 6 metal neighbors has further increased this interest.[3,4,9,10] Typical synthetic strategies have involved the reduction

---

[†] Purdue University.

[‡] Indiana University.

(1) Camille and Henry Dreyfus Teacher-Scholar, 1985-1990. Fellow of the Alfred P. Sloan Foundation, 1986-1990.

(2) (a) Dewey, C. G.; Ellis, J. E.; Fjane, K. L.; Fahl, K. M. P.; Warrock, G. F. P. *Organometallics* **1983**, *2*, 388. (b) Warrock, G. F. P.; Ellis, J. E. *J. Am. Chem. Soc.* **1984**, *106*, 5016.

(3) (a) Cotton, F. A.; Falvello, L. R.; Najaar, R. C. *Inorg. Chem.* **1983**, *22*, 375. (b) Cotton, F. A.; Roth, W. J. *Inorg. Chem.* **1983**, *22*, 868. (c) Cotton, F. A.; Roth, W. J. *Inorg. Chem.* **1984**, *23*, 845. (d) Cotton, F. A.; Roth, W. J. *J. Am. Chem. Soc.* **1983**, *105*, 3734. (d) Cotton, F. A.; Roth, W. J. *J. Am. Chem. Soc.* **1984**, *106*, 4749.

0002-7863/89/1511-4742$01.50/0

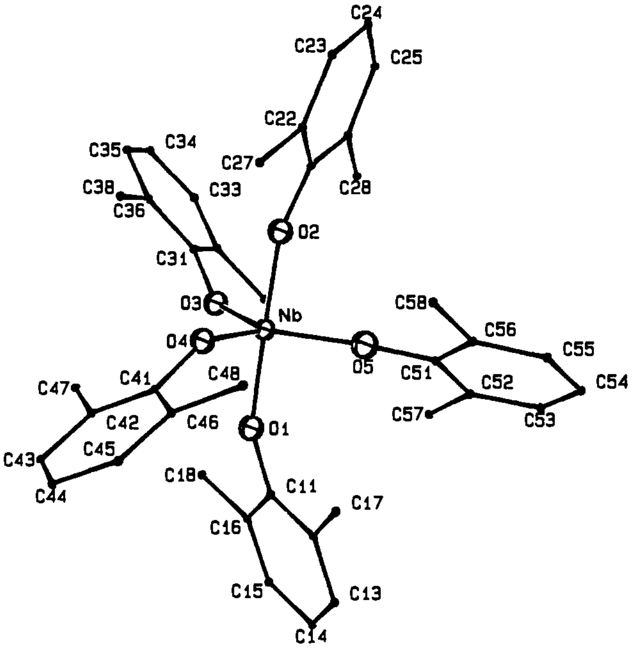

Figure 1. ORTEP view of $Nb(OAr\text{-}2,6Me_2)_5$ (**1c**) emphasizing the central coordination sphere.

of the pentahalides, MX_5 (M = Nb, Ta), normally in the presence of coordinating ligands such as tertiary phosphines or π-acid functionalities, and the resulting products are typically highly reducing substrates.

Table I. Fractional Coordinates and Isotropic Thermal Parameters for $Nb(OAr\text{-}2,6Me_2)_5$ (**1c**)

atom	10^4x	10^4y	10^4z	B_{iso}
Nb	53568 (2)	24457 (1)	67937 (1)	1.064 (5)
O1	6951 (2)	2507 (1)	7187 (1)	1.58 (4)
O2	3769 (2)	2329 (1)	6424 (1)	1.51 (4)
O3	5166 (2)	3570 (1)	7002 (1)	1.50 (4)
O4	5730 (2)	2260 (1)	5827 (1)	1.44 (4)
O5	5208 (2)	1641 (1)	7521 (1)	1.88 (5)
C11	7942 (2)	2337 (2)	7664 (2)	1.26 (6)
C12	8365 (2)	1534 (2)	7716 (2)	1.48 (6)
C13	9350 (3)	1380 (2)	8228 (2)	1.87 (7)
C14	9902 (3)	2000 (2)	8668 (2)	2.11 (7)
C15	9481 (3)	2796 (2)	8587 (2)	2.02 (7)
C16	8503 (2)	2978 (2)	8088 (2)	1.50 (6)
C17	7802 (3)	0870 (2)	7218 (2)	2.18 (7)
C18	8045 (3)	3837 (2)	7989 (2)	2.07 (7)
C21	2621 (2)	2173 (2)	6322 (2)	1.28 (6)
C22	2122 (2)	1794 (2)	5655 (2)	1.59 (6)
C23	0950 (3)	1643 (2)	5551 (2)	1.81 (6)
C24	0299 (3)	1862 (2)	6087 (2)	1.84 (6)
C25	0815 (3)	2232 (2)	6746 (2)	1.58 (6)
C26	1985 (3)	2386 (2)	6876 (2)	1.39 (6)
C27	2836 (3)	1579 (2)	5074 (2)	2.11 (7)
C28	2542 (3)	2776 (2)	7599 (2)	1.81 (6)
C31	4387 (2)	4204 (2)	6968 (2)	1.40 (6)
C32	4279 (3)	4592 (2)	7643 (2)	1.72 (6)
C33	3527 (3)	5254 (2)	7614 (2)	2.07 (7)
C34	2912 (3)	5523 (2)	6946 (2)	2.39 (7)
C35	3023 (3)	5120 (2)	6293 (2)	2.06 (7)
C36	3754 (3)	4453 (2)	6283 (2)	1.70 (6)
C37	4937 (3)	4303 (2)	8370 (2)	2.02 (7)
C38	3831 (3)	4043 (2)	5551 (2)	2.46 (7)
C41	6611 (2)	2239 (2)	5426 (2)	1.39 (6)
C42	7234 (3)	2952 (2)	5335 (2)	1.66 (6)
C43	8068 (3)	2905 (2)	4880 (2)	1.92 (7)
C44	8281 (3)	2185 (2)	4529 (2)	2.20 (7)
C45	7667 (3)	1487 (2)	4633 (2)	2.04 (7)
C46	6820 (3)	1496 (2)	5082 (2)	1.62 (6)
C47	6990 (3)	3754 (2)	5692 (2)	2.34 (7)
C48	6141 (3)	0746 (2)	5184 (2)	1.99 (7)
C51	5169 (2)	0962 (2)	7955 (2)	1.49 (6)
C52	5580 (3)	1020 (2)	8721 (2)	1.63 (6)
C53	5514 (3)	0323 (2)	9153 (2)	2.13 (7)
C54	5065 (3)	−0404 (2)	8835 (2)	2.33 (7)
C55	4684 (3)	−0448 (2)	8073 (2)	2.03 (7)
C56	4721 (2)	0237 (2)	7619 (2)	1.60 (6)
C57	6100 (3)	1802 (2)	9055 (2)	2.35 (7)
C58	4275 (3)	0202 (2)	6798 (2)	2.18 (7)

For the heavier group 6 metals molybdenum and tungsten, the elegant work of Chisholm et al. has shown that the presence of alkoxide ancillary ligands attached to multiply bonded dimetal centers is a powerful combination.[11,12] These compounds, exemplified by the dimers $M_2(OR)_6$ (M = Mo, W), exhibit a varied and high reactivity that is not demonstrated by any halide counterparts.[11,13] This enhanced reactivity of the midvalent alkoxides of Mo and W can be traced to the two critical characteristics of alkoxide ligands: strong oxygen-p to metal-d π-donation combined with a steric control of coordinate unsaturation. The ability of alkoxide ligands to π-donate to metal centers is most dramatically shown in structural studies of high-valent, electron-deficient alkoxide compounds.[14] The short M–O distances and large M–O–R angles normally found are typically ascribed to this effect. Besides a structural impact, the π-donation of alkoxide ligands has also been shown to have some dramatic spectroscopic manifestations.[15,16]

During our studies of the early transition-metal chemistry associated with aryloxide ligation, we have also observed the structural and chemical effects of the π-donor properties of these ligands.[17,18] Electrochemical studies of aryloxide derivatives of the early transition metals dramatically demonstrate the impact of oxygen-p to metal-d π-donation. Hence, for example, for a series of mixed chloro, aryloxides of titanium, $TiCl_n(OAr)_{4-n}$ (n = 2, 1, 0), the metal center becomes progressively more difficult

---

(4) (a) Sattelberger, A. P.; Wilson, R. B.; Huffman, J. C. *J. Am. Chem. Soc.* **1980**, *102*, 7111. (b) Leutkens, M. L.; Elcesser, W. L.; Huffman, J. C.; Sattelberger, A. P. *Inorg. Chem.* **1984**, *23*, 1718. (c) Leutkens, M. L.; Huffman, J. C.; Sattelberger, A. P. *J. Am. Chem. Soc.* **1985**, *107*, 3361. (d) Leutkens, M. L.; Santure, D. J.; Huffman, J. C.; Sattelberger, A. P. *J. Chem. Soc., Comm. Commun.* **1985**, 552.

(5) (a) Bellmonte, P. A.; Schrock, R. R.; Churchill, M. R.; Yourgs, W. J. *J. Am. Chem. Soc.* **1980**, *102*, 2858. (b) Rocklage, S. M.; Schrock, R. R. *J. Am. Chem. Soc.* **1982**, *104*, 3077. (c) Rocklage, S. M.; Turner, H. W.; Fellmann, J. D.; Schrock, R. R. *Organometallics* **1982**, *1*, 703.

(6) (a) Manzer, L. E. *Inorg. Chem.* **1977**, *16*, 525. (b) Tebbe, F. N. *J. Am. Chem. Soc.* **1973**, *95*, 5823. (c) Datta, S.; Wreford, S. S. *Inorg. Chem.* **1977**, *16*, 1134.

(7) (a) Neithamer, D. R.; Parkanyi, L.; Mitchell, J. F.; Wolczanski, P. T. *J. Am. Chem. Soc.* **1988**, *110*, 4421. (b) Lapointe, R. E.; Wolczanski, P. T.; Mitchell, J. F. *J. Am. Chem. Soc.* **1986**, *108*, 6832.

(8) (a) Cotton, F. A.; Hall, W. T. *J. Am. Chem. Soc.* **1979**, *101*, 5094. (b) Cotton, F. A.; Hall, W. T.; Cann, K. J.; Karl, F. J. *Macromolecules* **1981**, *14*, 233. (c) Bruck, M. A.; Copenhaver, A. S.; Wigley, D. E. *J. Am. Chem. Soc.* **1987**, *109*, 6525.

(9) (a) Ting, C.; Messerle, L. *J. Am. Chem. Soc.* **1987**, *109*, 6506. (b) Templeton, J. L.; McCarley, R. E. *Inorg. Chem.* **1978**, *17*, 2293. (c) Templeton, J. L.; Dorman, W. C.; Clardy, J. C.; McCarley, R. E. *Inorg. Chem.* **1978**, *17*, 1263.

(10) (a) Curtis, M. D.; Real, J. *J. Am. Chem. Soc.* **1986**, *108*, 4668. (b) Curtis, M. D.; Real, J. *Organometallics* **1985**, *4*, 940.

(11) (a) Chisholm, M. H. *Angew. Chem.* **1986**, *98*, 21. (b) Chisholm, M. H. *Polyhedron* **1986**, *5*, 25. (c) Chisholm, M. H. *J. Solid State Chem.* **1985**, *57*, 120.

(12) (a) Chisholm, M. H.; Hoffman, D. M.; Huffman, J. C. *Polyhedron* **1983**, *2*, 681.

(13) Cotton, F. A.; Walton, R. A. *Multiple Bonds between Metal Atoms*; Wiley and Sons: New York, 1982.

(14) Chisholm, M. H.; Rothwell, I. P. of *Comprehensive Coordination Chemistry*; Wilkinson, G., Gillard, R., McCleverty, J. A., Eds.; Pergamon Press: New York, 1987; Vol. 2, Chapter 15.3.

(15) Chisholm, M. H.; Huffman, J. C.; Rothwell, I. P.; Bradley, P. G.; Kress, N.; Woodruff, W. H. *J. Am. Chem. Soc.* **1981**, *103*, 4945.

(16) Chisholm, M. H.; Clark, D. L.; Kober, E. M.; Van Der Sluys, W. G. *Polyhedron* **1987**, *6*, 723.

(17) Rothwell, I. P. *Acc. Chem. Res.* **1988**, *21*, 153.

(18) (a) Durfee, L. D.; Kobriger, L. M.; McMullen, A. K.; Rothwell, I. P. *J. Am. Chem. Soc.* **1988**, *110*, 1463. (b) Kerschner, J. L.; Fanwick, P. E.; Rothwell, I. P. *J. Am. Chem. Soc.* **1987**, *109*, 5840. (c) Fanwick, P. E.; Ogilvy, A. E.; Rothwell, I. P. *Organometallics* **1987**, *6*, 73. (d) Latesky, S. L.; McMullen, A. K.; Rothwell, I. P.; Huffman, J. C. *Organometallics* **1985**, *4*, 902.

Table II. Selected Bond Distances (Å) and Angles (deg) for $Nb(OAr\text{-}2,6Me_2)_5$ (**1c**)

Nb–O(1)	1.910 (2)	Nb–O(2)	1.901 (2)
Nb–O(3)	1.893 (2)	Nb–O(4)	1.903 (2)
Nb–O(5)	1.890 (2)		
O(1)–Nb–O(2)	176.98 (8)	O(3)–Nb–O(4)	113.05 (9)
O(1)–Nb–O(3)	91.06 (8)	O(3)–Nb–O(5)	120.35 (9)
O(1)–Nb–O(4)	89.27 (8)	O(4)–Nb–O(5)	126.58 (9)
O(1)–Nb–O(5)	88.58 (8)	Nb–O(1)–C(11)	157.0 (2)
O(2)–Nb–O(3)	91.37 (8)	Nb–O(2)–C(21)	166.5 (2)
O(2)–Nb–O(4)	91.45 (8)	Nb–O(3)–C(31)	144.8 (2)
O(2)–Nb–O(5)	88.64 (8)	Nb–O(4)–C(4)	143.8 (2)
		Nb–O(5)–C(51)	169.3 (2)

Table III. Fractional Coordinates and Isotropic Thermal Parameters for $Nb(OAr\text{-}4Me)_2(dmpe)_2$ (**2a**)

atom	10^4x	10^4y	10^4z	B_{iso}
Nb(1)A	0*	0*	0*	13
P(2)A	−996 (1)	−420 (1)	−2747 (1)	17
P(3)A	709 (1)	1921 (1)	−1094 (1)	16
C(4)A	−1213 (4)	410 (4)	−3914 (6)	28
C(5)A	−2399 (4)	−718 (4)	−3122 (6)	29
C(6)A	−267 (4)	−1646 (4)	−3891 (5)	24
C(7)A	15 (4)	−2447 (4)	−3086 (5)	23
C(8)A	563 (4)	−2882 (4)	−321 (6)	25
C(9)A	2167 (4)	−2271 (4)	−1258 (6)	24
O(10)A	1264 (2)	371 (2)	−513 (4)	21
C(11)A	1989 (3)	595 (3)	−1052 (5)	15
C(12)A	3103 (4)	113 (3)	−858 (5)	19
C(13)A	3870 (4)	350 (4)	−1431 (5)	21
C(14)A	3576 (4)	1070 (4)	−2200 (5)	20
C(15)A	2479 (4)	1559 (4)	−2364 (5)	21
C(16)A	1694 (4)	1325 (3)	−1820 (5)	18
C(17)A	4423 (4)	1332 (5)	−2799 (6)	33
Nb(1)B	5000*	5000*	5000*	12
P(2)B	4215 (1)	3430 (1)	2987 (1)	16
P(3)B	6234 (1)	3469 (1)	5779 (1)	17
C(4)B	4833 (4)	2985 (4)	1320 (5)	25
C(5)B	2753 (4)	3282 (4)	2112 (5)	23
C(6)B	4669 (4)	2292 (4)	3682 (6)	24
C(7)B	5903 (4)	2202 (4)	4405 (6)	26
C(8)B	6171 (4)	3313 (4)	7544 (6)	26
C(9)B	7739 (4)	3305 (4)	5931 (6)	27
O(10)B	6085 (2)	4842 (2)	3711 (3)	21
C(11)B	6843 (4)	5122 (3)	3267 (5)	17
C(12)B	7897 (4)	5262 (3)	4182 (5)	18
C(13)B	8684 (4)	5529 (3)	3695 (5)	20
C(14)B	8473 (4)	5657 (3)	2288 (5)	20
C(15)B	7430 (4)	5509 (4)	1376 (5)	21
C(16)B	6623 (4)	5244 (4)	1834 (5)	20
C(17)B	9362 (4)	5927 (4)	1778 (6)	28

Table IV. Selected Bond Distances (Å) and Angles (deg) for $Nb(OAr\text{-}4Me)_2(dmpe)_2$ (**2a**)

	molecule A	molecule B
Nb–P(2)	2.539 (2)	2.662 (2)
Nb–P(3)	2.552 (2)	2.555 (2)
Nb–O(10)	2.022 (3)	2.023 (3)
P(2)–Nb–P(3)	103.18 (5)	103.42 (5)
P(2)–Nb–O(10)	90.1 (1)	88.2 (1)
P(3)–Nb–O(10)	89.5 (1)	87.37 (9)
Nb–O(10)–C(11)	171.3 (3)	156.4 (3)

to reduce by ≈250–350 mV on substituting one aryloxide for a chloride ligand.[19] This contrasts with the much smaller change of ≈50 mV on moving through the halogen elements (Cl, Br, I). This effect is also seen for the mixed halo, aryloxides of W(VI).[20,21] Similarly this stabilization of high-valent metals by π-donor alkoxide or aryloxide ligation contrasts with the destabilizing effect these ligands have when attached to low-valent metal centers. In the quadruply bonded $Mo_2X_4(PMe_3)_4$ derivatives electrochemical studies show aryloxide ligands to increase the ease of oxidation of the Mo_2^{4+} core dramatically over their halide counterparts.[22] The destabilization of the HOMO, δ-orbital by the π-donating oxygen donor ligand is also evident in spectroscopic and structural studies.[16,22]

In this paper we report the synthesis of a series of mononuclear niobium compounds containing aryloxide ligation. The emphasis of this particular contribution involves the isolation of compounds containing the metal in as wide a range of formal oxidation states as possible in order to evaluate how the characteristics of metal–aryloxide bonding vary with this particular parameter.

Results and Discussion

Our initial synthetic strategy for the synthesis of lower valent aryloxide compounds of niobium has been the reduction of a series of pentaphenoxides in the presence of bis(dimethylphosphino)ethane (dmpe). The three homoleptic aryloxides $Nb(OAr)_5$ (OAr = OAr-4Me, 4-methylphenoxide, **1a**; $OAr\text{-}3,5Me_2$, 3,5-dimethylphenoxide, **1b**; $OAr\text{-}2,6Me_2$, 2,6-dimethylphenoxide, **1c**)[23] have been synthesized as substrates for reduction. In the case of the less bulky aryloxides OAr-4Me and $OAr\text{-}3,5Me_2$ the compounds exist as dimers, while in the case of the more bulky 2,6-dimethylphenoxide ($OAr\text{-}2,6Me_2$) the simple five-coordinate monomer appears stable toward dimerization. This was confirmed by a single-crystal X-ray analysis of $Nb(OAr\text{-}2,6Me_2)_5$ (**1c**) (Figure 1). Although there have been structural studies of dimeric alkoxides or phenoxides of Nb and Ta,[24] this appears to be the first structurally studied monomer of the type $M(OR)_5$ or $M(OAr)_5$. The structural parameters of this molecule are also of importance in this particular study for comparison with reduced derivatives (vide infra). Table I contains the fractional coordinates and isotropic parameters, while Table II contains some selected bond distances and angles. The coordination environment about the niobium atom can be seen to be almost perfectly trigonal-bipyramidal (Figure 1). The only other homoleptic, five-coordinate compound of niobium that has been reported is $Nb(NMe_2)_5$.[25] Here a geometry much closer to a square-based pyramid was found. However, predicting and even rationalizing which of these two extreme geometries will be formed is not straightforward, especially for sterically noninnocent ligands.[26]

Electrochemical studies of the three pentaaryloxides in THF with $Bu_4{}^nN^+PF_6^-$ as the supporting electrolyte indicated the presence in all cases of a reasonably accessible, irreversible, one-electron reduction at potentials of −1.4 to −1.5 V vs a silver quasi-reference electrode ($Cp_2Fe^{0/+}$ = +0.47 V). This compares with much more negative values of $E_{p,c}$ for $Ta(OAr\text{-}2,6Me_2)_5$, −2.25 V, and $Nb(OPr^i)_5$, −2.51 V.[27] The bulk reduction of toluene solutions of the aryloxides $Nb_2(OAr\text{-}4Me)_{10}$ (**1a**) and $Nb_2(OAr\text{-}3,5Me_2)_{10}$ (**1b**) with sodium amalgam (3 Na per Nb) in the presence of dmpe takes place according to eq 1.

$$\underset{\mathbf{1}}{Nb_2(OAr)_{10}} + 6Na + 4dmpe \rightarrow \underset{\mathbf{2}}{2Nb(OAr)_2(dmpe)_2} + 6NaOAr \quad (1)$$

a; OAr = OAr-4Me, **b**; OAr = $OAr\text{-}3,5Me_2$

---

(19) (a) Latesky, S. L.; McMullen, A. K.; Keddington, J.; Rothwell, I. P.; Huffman, J. C. *Inorg. Chem.* **1985**, *24*, 995. (b) Durfee, L. D.; Rothwell, I. P.; Huffman, J. C. *Inorg. Chem.* **1985**, *24*, 4569.

(20) Beshouri, S.; Rothwell, I. P. *Inorg. Chem.* **1986**, *25*, 1962.

(21) In order for the argument to be correct, the molecular symmetry must allow π-donation into the metal-based LUMO's.

(22) Coffindaffer, T. W.; Niccolai, G.; Powell, D.; Rothwell, I. P.; Huffman, J. C. *J. Am. Chem. Soc.* **1985**, *107*, 3572.

(23) (a) Chamberlain, L. R.; Rothwell, I. P.; Huffman, J. C. *Inorg. Chem.* **1984**, *23*, 2575. (b) Funk, V. H.; Baumann, W. *Z. Anorg. Allg. Chem.* **1937**, 231, 264.

(24) (a) Wang, R.; Folting, K.; Huffman, J. C.; Chamberlain, L. R.; Rothwell, I. P. *Inorg. Chim. Acta* **1983**, *120*, 81. (b) Lewis, L. N.; Garbauskas, M. E. *Inorg. Chem.* **1985**, *24*, 363.

(25) Heath, C.; Hursthouse, M. B. *J. Chem. Soc., Chem. Commun.* **1971**, 143.

(26) Chisholm, M. H.; Tan, L.-S.; Huffman, J. C. *J. Am. Chem. Soc.* **1982**, *104*, 4879.

(27) Coffindaffer, T. W.; Rothwell, I. P., unpublished results.

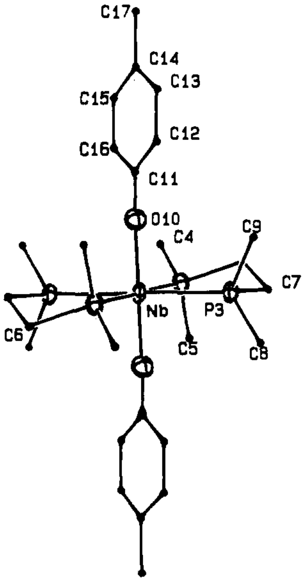

Figure 2. ORTEP view of $Nb(OAr\text{-}4Me)_2(dmpe)_2$ (**2a**) emphasizing the central coordination sphere.

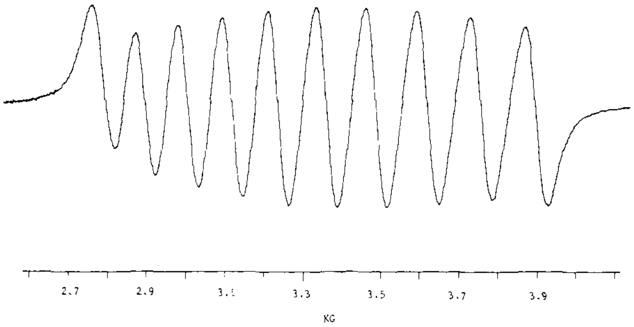

Figure 3. X-band ESR spectrum of $Nb(OAr\text{-}4Me)_2(dmpe)_2$ (**2a**) in toluene solution at 25 °C.

The initially clear yellow solutions rapidly become green with the formation of a sparingly soluble green powder (vide infra). As the reaction proceeds the solution darkens, resulting in a deep brown final mixture. Workup involving filtration, partial removal of solvent, and slow cooling gave the bis-aryloxides (**2**) as large, purple crystals in yields of 30–35%. The brown supernatant contained significant amounts of **2**, as evidenced from ESR spectra, contaminated by other unidentified products. A single-crystal X-ray diffraction study of **2a** confirmed the stoichiometry (Figure 2). Fractional coordinates and isotropic thermal parameters are contained in Table III, while Table IV contains some pertinent bond distances and angles. The six-coordinate niobium atom lies on a crystallographic inversion center surrounded by two trans oxygen atoms and four phosphorus atoms. The crystal was found to contain two independent molecules in the unit cell. The only significant difference between the two molecules is the value for the Nb–O–Ar angle of 156.4 (3)° and 171.3 (3)°, respectively. Spectroscopically these d^3-molecules exhibit characteristic ESR spectra (Figure 3) consisting of the ten lines expected for a metal-based (Nb, $I = 9/2$) radical. These spectra combined with solution magnetic moments of 1.05 and 1.10 μ_B for **2a** and **2b** are consistent with a doublet, low-spin electron configuration (vide infra). Both structurally and spectroscopically these molecules are closely related to the dichlorides $MCl_2(dmpe)_2$ (M = Nb, Ta) reported by Sattleberger et al.[4]

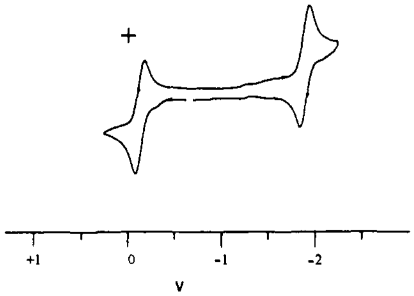

Figure 4. Cyclic voltamogram of $Nb(OAr\text{-}4Me)_2(dmpe)_2$ (**2a**) in THF/TBAH (0.2 M) using a Pt disc electrode and 50 mV/s sweep rate. Potentials are vs an Ag pseudoreference electrode against which the $Cp_2Fe^{0/+}$ wave appears at +0.47 V.

Electrochemical studies (cyclic voltametry and coulometry) of both **2a** and **2b** show the presence of two waves in the cyclic voltammogram. The first, very accessible wave corresponds to a one-electron oxidation occurring at −0.09 V, while the second one-electron reduction takes place at −1.81 V (Figure 4). Both waves appear to be reversible as measured by the criteria that ipa/ipc = 1 even at slow scan rates, while the separation of the anodic and cathodic peaks is similar to that of the $Cp_2Fe^{0/+}$ couple under identical conditions. However, only the oxidation wave is actually chemically reversible. Hence, bulk electrochemical oxidation at 0 V produces, after the passage of 1 equiv of electrons, light green solutions which exhibit an identical cyclic voltammogram to that of **2** except that the wave at −0.09 V is now a reduction. Bulk electrochemical reduction of these green solutions then regenerates solutions of **2** typically in 80–90% yield as judged by the overall decay in the cyclic voltammogram. This data is, therefore, consistent with the presence of the reversible couple shown.

$$\underset{\mathbf{2}}{Nb(OAr)_2(dmpe)_2} \rightleftarrows Nb(OAr)_2(dmpe)_2^+ + e^-$$

Carrying out bulk electrochemical reduction of solutions of **2** at the potentials negative of the second wave (−2.0 V) resulted in dark solutions whose cyclic voltammograms were entirely different from those of **2**. Hence the presumed intermediate monoanion $[Nb(OAr)_2(dmpe)_2]^-$ appears to be unstable.

Attempts to produce the monocation by chemical methods met with mixed success. Hence the addition of the mild oxidizing agent $Ag^+PF_6^-$ to THF solutions of **2** did indeed yield green solutions once the metallic silver produced had been removed. Removal of solvent yielded a greenish solid whose cyclic voltammogram was identical with that of **2** except that both waves were now reductions. However, attempts to purify this product proved difficult, particularly due to its tendency to decompose slowly over time in the solid state and in solution.

Stable derivatives of this monocation were obtained unexpectedly by an alternative oxidation process. It has been shown by Sattelberger et al. that the dichloride derivatives $NbCl_2(dmpe)_2$ will undergo facile oxidative–addition of dihydrogen to generate Nb(IV) hydride compounds.[4] We, therefore, attempted to oxidatively add phenols to the compounds of type **2** in the hope of generating mixed hydride, aryloxides. However, the reaction of **2** with the parent phenols was found to lead to a non-hydride-containing product **3** of stoichiometry "$Nb(OAr)_4(dmpe)$" and H_2 gas. Spectroscopic data for **3** was found to be entirely inconsistent with its formulation as containing a Nb(IV), d^1-metal center. Instead the identity of **3** as a mixed salt compound of formula $[Nb(OAr)_2(dmpe)_2]^+[Nb(OAr)_6]^-$ was strongly indicated by its spectroscopic data and confirmed by a single-crystal X-ray diffraction analysis of **3b**. An ORTEP view of the cation and anion in **3b** is shown in Figures 5 and 6, respectively, while Tables V and VI contain fractional coordinates and selected bond distances and angles. The octahedral, hexaphenoxide anion in **3b** (Figure 6) contains little of special note. However, the monocation (Figure 5) corresponds with the species identified in the electrochemical studies as the one-electron oxidation product of **2b**. Indeed the cyclic voltammograms of **3b** show two one-electron reduction waves at position corresponding to those seen for the oxidation and reduction wave in **2b** superimposed on a new reduction which is presumably due to the anion. The structure of the cation can be seen to be closely related to that of **2** with trans axial aryloxide ligands and equational dmpe chelates (Figure 5). However, an intriguing difference concerns the mutual orientation of the aryl

Table V. Fractional Coordinates and Isotropic Thermal Parameters for $[Nb(OAr\text{-}3,5Me_2)_2(dmpe)_2][Nb(OAr\text{-}3,5Me_2)_6]$ (**3b**)

atom	10^4x	10^4y	10^4z	B_{iso}	atom	10^4x	10^4y	10^4z	B_{iso}
Nb(1)	5699 (1)	2304 (1)	4488 (1)	14	O(46)	2362 (5)	3704 (5)	−387 (10)	21
P(2)	6588 (2)	2623 (2)	6286 (4)	16	C(47)	2616 (8)	3884 (8)	−958 (17)	17 (4)
C(3)	7186 (7)	2353 (8)	6230 (15)	22 (4)	C(48)	3184 (7)	3722 (8)	−558 (16)	13 (4)
C(4)	7093 (8)	2400 (8)	4970 (16)	26 (4)	C(49)	3421 (8)	3958 (8)	−1189 (16)	17 (4)
P(5)	6444 (2)	2007 (2)	3974 (4)	19	C(50)	3158 (8)	4312 (8)	−2133 (16)	16 (4)
C(6)	6703 (8)	3390 (9)	6398 (17)	30 (4)	C(51)	2589 (8)	4446 (9)	−2520 (17)	22 (4)
C(7)	6715 (8)	2404 (8)	7715 (16)	24 (4)	C(52)	2336 (8)	4229 (8)	−1920 (17)	18 (4)
C(8)	6401 (7)	2106 (8)	2547 (15)	21 (4)	C(53)	4039 (9)	3776 (9)	−762 (18)	28 (5)
C(9)	6669 (8)	1269 (8)	4366 (17)	27 (4)	C(54)	2267 (8)	4828 (9)	−3580 (17)	21 (4)
P(10)	4985 (2)	2616 (2)	5064 (4)	22	O(55)	2605 (5)	2785 (5)	2302 (10)	22
C(11)	4280 (9)	2634 (10)	3757 (19)	38 (5)	C(56)	2915 (7)	2704 (8)	3442 (15)	10 (3)
C(12)	4230 (9)	2089 (10)	3038 (20)	42 (5)	C(57)	2989 (8)	2141 (9)	3844 (17)	23 (4)
P(13)	4777 (2)	2031 (2)	2680 (4)	25	C(58)	3295 (8)	2051 (9)	5044 (17)	22 (4)
C(14)	5012 (8)	3323 (9)	5735 (17)	31 (4)	C(59)	3533 (8)	2527 (8)	5833 (17)	21 (4)
C(15)	4902 (9)	2132 (9)	6046 (19)	39 (5)	C(60)	3425 (8)	3077 (9)	5380 (17)	22 (4)
C(16)	4639 (9)	1327 (10)	2002 (19)	38 (5)	C(61)	3118 (7)	3168 (8)	4194 (15)	13 (4)
C(17)	4576 (9)	2503 (10)	1421 (19)	42 (5)	C(62)	3376 (10)	1445 (11)	5529 (21)	43 (6)
O(18)	5738 (5)	1577 (5)	5179 (10)	20	C(63)	3649 (9)	3581 (10)	6224 (19)	31 (5)
C(19)	5755 (7)	1047 (8)	5611 (16)	22 (4)	O(64)	2082 (5)	3833 (5)	1325 (10)	26
C(20)	5879 (7)	993 (8)	6758 (15)	19 (4)	C(65)	1971 (8)	4248 (9)	1899 (18)	23 (4)
C(21)	5900 (7)	456 (7)	7199 (15)	17 (3)	C(66)	1404 (8)	4361 (9)	1519 (17)	18 (4)
C(22)	5817 (7)	−23 (8)	6495 (15)	20 (4)	C(67)	1299 (8)	4776 (8)	2104 (16)	18 (4)
C(23)	5714 (7)	24 (8)	5410 (15)	19 (4)	C(68)	1711 (9)	5084 (9)	3048 (19)	29 (5)
C(24)	5677 (7)	580 (8)	4914 (15)	20 (4)	C(69)	2266 (8)	4957 (9)	3356 (17)	19 (4)
C(25)	6053 (8)	378 (9)	8473 (18)	33 (4)	C(70)	2405 (9)	4549 (9)	2796 (19)	28 (5)
C(26)	5603 (8)	−502 (9)	4606 (18)	31 (4)	C(71)	701 (9)	4929 (10)	1736 (20)	34 (5)
O(27)	5646 (5)	3045 (5)	3802 (10)	19	C(72)	2746 (9)	5277 (9)	4352 (18)	28 (5)
C(28)	5638 (7)	3499 (8)	3195 (15)	20 (4)	O(73)	1800 (5)	2836 (5)	71 (10)	19
C(29)	5203 (7)	3883 (8)	2792 (15)	20 (4)	C(74)	1279 (7)	2720 (8)	−259 (14)	10 (3)
C(30)	5192 (7)	4355 (8)	2152 (15)	21 (4)	C(75)	1122 (8)	2164 (8)	−330 (16)	16 (4)
C(31)	5628 (8)	4451 (8)	1944 (16)	24 (4)	C(76)	571 (8)	2011 (9)	−662 (16)	18 (4)
C(32)	6066 (8)	4067 (8)	2329 (16)	25 (4)	C(77)	184 (8)	2456 (8)	−928 (16)	18 (4)
C(33)	6084 (7)	3583 (8)	3007 (15)	22 (4)	C(78)	331 (8)	3006 (9)	−917 (17)	21 (4)
C(34)	4712 (8)	4783 (9)	1701 (17)	29 (4)	C(79)	883 (8)	3143 (9)	−569 (17)	22 (4)
C(35)	6530 (9)	4133 (9)	2087 (18)	36 (5)	C(80)	401 (9)	1382 (10)	−737 (19)	31 (5)
Nb(36)	2479 (1)	3261 (1)	964 (1)	14	C(81)	−80 (11)	3495 (11)	−1213 (22)	50 (6)
O(37)	2869 (5)	2697 (5)	565 (10)	20	O(82)	3171 (5)	3655 (5)	1925 (10)	23
C(38)	2931 (8)	2162 (8)	329 (16)	15 (4)	C(83)	3437 (8)	4147 (9)	2361 (17)	19 (4)
C(39)	3134 (7)	2072 (8)	−443 (16)	15 (4)	C(84)	3815 (8)	4191 (8)	3576 (16)	15 (4)
C(40)	3203 (8)	1516 (9)	−706 (18)	23 (5)	C(85)	4067 (8)	4695 (9)	4050 (17)	22 (4)
C(41)	3082 (9)	1049 (10)	−180 (18)	28 (5)	C(86)	3964 (8)	5197 (9)	3358 (17)	23 (4)
C(42)	2882 (9)	1152 (10)	580 (18)	27 (5)	C(87)	3606 (8)	5138 (8)	2156 (17)	18 (4)
C(43)	2806 (8)	1690 (9)	839 (16)	19 (4)	C(88)	3326 (8)	4630 (8)	1653 (16)	16 (4)
C(44)	3406 (9)	1387 (10)	−1558 (19)	34 (5)	C(89)	4435 (8)	4765 (9)	5347 (17)	21 (4)
C(45)	2791 (10)	645 (10)	1203 (20)	40 (6)	C(90)	3500 (9)	5655 (10)	1392 (19)	33 (5)

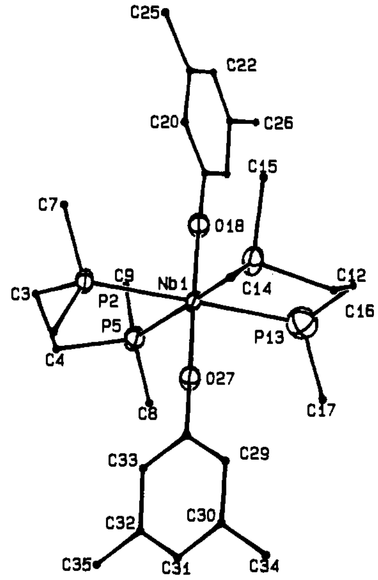

Figure 5. ORTEP view of the cation $[Nb(OAr\text{-}3,5Me_2)_2(dmpe)_2]^+$ contained in **3b**.

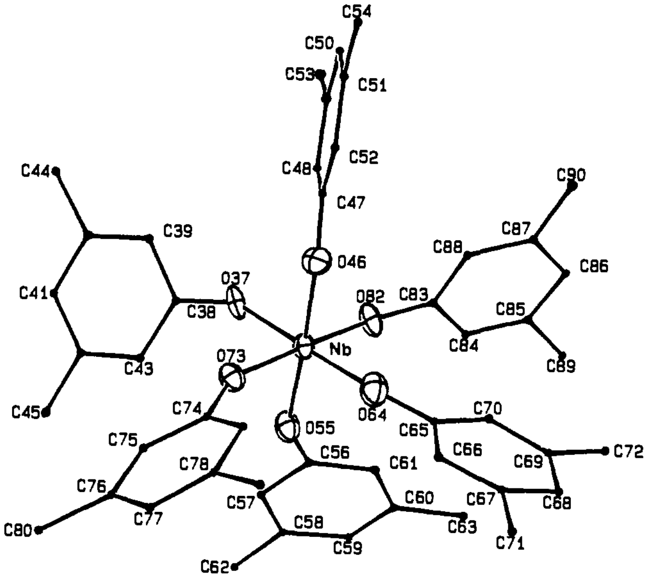

Figure 6. ORTEP view of the anion $[Nb(OAr\text{-}3,5Me_2)_6]^-$ contained in **3b**.

groups of the two aryloxide ligands. In the neutral compound **2a** these groups are coplanar, while in the cation of **3b** they are perpendicular to each other (Figures 2 and 6). Unlike their alkoxide counterparts, aryloxide and siloxide[7,28] ligands have the ability for their oxygen atoms to π-interact with their substituents as well as the metal atom to which they are bound. This feature has been used to rationalize the very large, sometimes linear

Table VI. Selected Bond Distances (Å) and Angles (deg) for $[Nb(OAr\text{-}3,5Me_2)_2(dmpe)_2][Nb(OAr\text{-}3,5Me_2)_6]$ (**3b**)

$[Nb(OAr\text{-}3,5Me_2)_2(dmpe)_2]^+$			
Nb(1)–P(2)	2.563 (3)	Nb(1)–P(5)	2.591 (3)
Nb(1)–P(10)	2.577 (3)	Nb(1)–P(13)	2.589 (3)
Nb(1)–O(18)	1.917 (2)	Nb(1)–O(27)	1.937 (2)
O(18)–Nb(1)–O(27)	178.5 (1)	P(2)–Nb(1)–P(13)	177.0 (1)
P(5)–Nb(1)–P(10)	178.03 (8)	Nb(1)–O(18)–C(19)	176.83 (6)
Nb(1)–O(27)–C(28)	168.54 (6)		
$[Nb(OAr\text{-}3,5Me_2)_6]^-$			
Nb(36)–O(37)	1.95 (1)	Nb(36)–O(46)	1.96 (1)
Nb(36)–O(55)	1.98 (1)	Nb(36)–O(64)	1.95 (1)
Nb(36)–O(73)	1.94 (1)	Nb(36)–O(82)	1.95 (1)
O(37)–Nb(36)–O(64)	178.5 (6)	O(73)–Nb(36)–O(82)	176.9 (6)
O(46)–Nb(36)–O(55)	177.6 (6)	Nb(36)–O(37)–C(38)	149.6 (1)
Nb(36)–O(46)–C(47)	142.6 (1)	Nb(36)–O(55)–C(36)	145.8 (1)
Nb(36)–O(64)–C(65)	161.0 (1)	Nb(36)–O(73)–C(74)	152.7 (1)
Nb(36)–O(82)–C(83)	148.5 (1)		

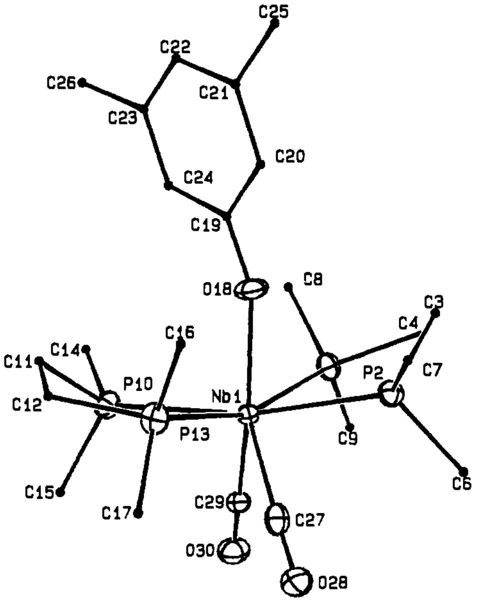

Figure 7. ORTEP view of $Nb(OAr\text{-}3,5Me_2)(CO)_2(dmpe)_2$ (**4b**) emphasizing the central coordination sphere.

M–O–Ar and $M\text{–}O\text{–}SiR_3$ angles typically found for high-valent, electron-deficient metal aryloxides[29] and siloxides.[7,28] If one considers the case of a linear M–O–X function, the sp-hybridized oxygen atom has two mutually perpendicular p-orbitals which can π-donate to empty d-orbitals of the correct symmetry on the metal. In the case of an aryloxide ligand, one of the p-orbitals can overlap with the arene ring, reducing its availability for interaction with the metal. Hence, one might rationalize from this simple picture that the strongest π-donation from aryloxide ligands should occur into metal d-orbitals which are coplanar with the aryl ring. If this is indeed the case, then the orientation of the aryl rings in the absence of dominating steric effect may give some insight into the oxygen-p to metal-d π-bonding.[29]

In both of the six coordinate compounds **2a** and **3b** the trans axial aryloxide ligands can π-donate into the d_{xz}, d_{yz} pair of orbitals. However, in the case of the low spin d^3-neutral **2a** one of these orbitals must contain the unpaired electron, with the other two electrons occupying the lowest lying d_{xy} orbital. The energy of the unpaired electron will be increased as π-donation takes place into the d_{xz} orbital. If one considers the coplanar orientation of the aryl rings in **2a**, then this indicates, based on the preceding argument, that both ligands are π-donating more strongly into the same metal orbital, presumably the one that does not contain the unpaired electron. In the d^2-monocation **3b** the mutual perpendicular orientation of the aryl rings implies equal π-donation is taking place into both the d_{xz} and d_{yz} orbitals. The electronic rationalization of the orientations of aryloxide aryl rings in this fashion can be related to similar arguments used for dialkylamido ligands,[30] although the effects are expected to be much less dramatic.

Table VII. Fractional Coordinates and Isotropic Thermal Parameters for $Nb(OAr\text{-}3,5Me_2)(CO)_2(dmpe)_2$ (**4b**)

atom	10^4x	10^4y	10^4z	B_{iso}
Nb(1)	3150.3 (3)	1473.4 (4)	3656.0 (2)	10
P(2)	4333 (1)	1541 (1)	4256 (1)	14
C(3)	4077 (4)	821 (6)	4826 (2)	22
C(4)	3300 (4)	1298 (7)	5023 (3)	25
P(5)	2544 (1)	1509 (1)	4535 (1)	15
C(6)	4693 (4)	2855 (6)	4480 (3)	23
C(7)	5253 (4)	839 (6)	4073 (3)	21
C(8)	1833 (5)	392 (6)	4661 (3)	25
C(9)	2013 (4)	2709 (6)	4767 (2)	22
P(10)	1946 (1)	984 (1)	3092 (1)	16
C(11)	2231 (5)	−65 (8)	2640 (3)	41
C(12)	2994 (5)	200 (9)	2413 (3)	52
P(13)	3746 (1)	790 (1)	2830 (1)	18
C(14)	1022 (5)	402 (8)	3337 (3)	37
C(15)	1548 (5)	2074 (7)	2718 (3)	40
C(16)	4500 (5)	−281 (6)	2890 (3)	29
C(17)	4233 (5)	1724 (7)	2399 (3)	40
O(18)	3308 (3)	−249 (3)	3863 (2)	20
C(19)	3219 (4)	−1327 (5)	3865 (2)	18
C(20)	3881 (4)	−2021 (5)	3955 (2)	17
C(21)	3800 (4)	−3162 (5)	3964 (2)	18
C(22)	3055 (4)	−3631 (5)	3876 (2)	18
C(23)	2398 (4)	−2982 (5)	3780 (2)	18
C(24)	2488 (4)	−1853 (5)	3776 (2)	20
C(25)	4516 (5)	−3892 (6)	4072 (3)	28
C(26)	1581 (4)	−3488 (6)	3678 (3)	25
C(27)	3791 (4)	2790 (5)	3434 (2)	16
O(28)	4178 (3)	3560 (4)	3315 (2)	22
C(29)	2506 (4)	2888 (5)	3634 (2)	13
O(30)	2138 (3)	3707 (3)	3622 (2)	22

Table VIII. Selected Bond Distances (Å) and Angles (deg) for $Nb(OAr\text{-}3,5Me_2)(CO)_2(dmpe)_2$ (**4a**)

Nb–P(2)	2.572 (2)	Nb–O(18)	2.181 (4)
Nb–P(5)	2.608 (2)	Nb–C(27)	2.019 (6)
Nb–P(10)	2.608 (2)	Nb–C(29)	2.028 (6)
Nb–P(13)	2.603 (2)	C(27)–O(28)	1.181 (7)
C(29)–O(30)	1.169 (7)		
P(2)–Nb–P(5)	73.31 (6)	P(5)–Nb–P(10)	104.30 (6)
P(2)–Nb–P(10)	168.44 (10)	P(5)–Nb–P(13)	162.37 (6)
P(2)–Nb–P(13)	105.48 (6)	P(5)–Nb–O(18)	79.9 (1)
P(2)–Nb–O(18)	76.8 (1)	P(5)–Nb–C(27)	118.1 (2)
P(2)–Nb–C(27)	75.9 (1)	P(5)–Nb–C(29)	78.8 (2)
P(2)–Nb–C(29)	113.7 (2)		
P(10)–Nb–P(13)	73.24 (6)	P(13)–Nb–O(18)	82.7 (1)
P(10)–Nb–O(18)	91.6 (1)	P(13)–Nb–C(27)	77.7 (2)
P(10)–Nb–C(27)	114.4 (2)	P(13)–Nb–C(29)	116.6 (2)
P(10)–Nb–C(29)	76.3 (2)	C(27)–Nb–C(29)	66.7 (2)
O(18)–Nb–C(77)	140.6 (2)	Nb–C(27)–O(28)	178.1 (5)
O(18)–Nb–C(29)	151.9 (2)	Nb–C(29)–O(30)	179.6 (5)
Nb–O(18)–C(19)	159.9 (4)		

The formation of the mixed-valence salt **3b** instead of the simple neutral $[Nb(OAr\text{-}3,5Me_2)_4(dmpe)]$ is somewhat puzzling. The one-electron reduction of $Nb_2(OAr\text{-}3,5Me_2)_{10}$ in the presence of dmpe was found to consistently generate green solutions of **3b**. However, there is precedence in molybdenum alkoxide chemistry for chelating ligation to be able to sometimes induce disproportionation reactions.[15a]

---

(28) (a) Chisholm, M. H.; Reichert, W. W.; Thornton, P. *J. Am. Chem. Soc.* **1978**, *100*, 2744. (b) Chisholm, M. H.; Felton, F. A.; Ectine, M. W.; Reichert, W. W. *Inorg. Chem.* **1978**, *17*, 2944.

(29) Coffindaffer, T. W.; Rothwell, I. P.; Huffman, J. C. *Inorg. Chem.* **1983**, *22*, 2906.

(30) Chisholm, M. H.; Extine, M. W.; Cotton, F. A.; Stults, B. R. *J. Am. Chem. Soc.* **1976**, *98*, 4477.

Table IX. Variation of Nb-OAr Distance and Nb-O-Ar angle with Metal Electron Configuration

compd	formal Nb oxidation state	electron count[a]	Nb-O (Å)	Nb-O-Ar (deg)
$Nb(OAr\text{-}2,6Me_2)_5$	+5	10	1.890 (2)–1.910 (2)	143.8 (2)–169.3 (2)
$[Nb(OAr\text{-}3,5Me_2)_6]^-$	+5	12	1.95 (1)–1.98 (1)	142.6 (1)–161.0 (1)
$[Nb(OAr\text{-}3,5Me_2)_2(dmpe)_2]^+$	+3	14	1.917 (2), 1.937 (2)	168.6 (1), 176.8 (1)
$Nb(OAr\text{-}4Me)_2(dmpe)_2$	+2	15	2.022 (3), 2.023 (3)	156.4 (3), 171.3 (3)
$Nb(OAr\text{-}3,5Me_2)(CO)_2(dmpe)_2$	+1	18	2.181 (4)	159.9 (4)

[a] About the metal assuming no π-donation.

A deep purple solution of the Nb(II) compound **2b** was also found to react rapidly with carbon monoxide. Hence lightening to dark orange was found on exposing toluene solutions of **2b** to an atmosphere of CO gas. From these solutions orange crystals of the 18-electron dicarbonyl $Nb(OAr\text{-}3,5\text{-}Me_2)(CO)_2(dmpe)_2$ (**4b**) were obtained in ≈50% yield. A much higher yield of **4b** was achieved by reducing $Nb(OAr\text{-}3,5Me_2)_5$ in the presence of dmpe (2 equiv) and CO using sodium amalgam (4 Na per Nb). Compound **4b** represents an example of a now large class of seven-coordinate compounds of stoichiometry $XM(CO)_2(L)_4$ (X = anionic ligand, e.g., H, Cl, R; M = Nb, Ta).[6,31] A solid-state X-ray diffraction analysis of **4b** also showed it to be structurally related. An ORTEP view of **4b** is shown in Figure 7, while Tables VII and VIII contain fractional coordinates and selected bond distances and angles, respectively. The structure of **4b** is best described as monocapped trigonal prismatic, with the aryloxide ligand as the capping group. The two carbonyl groups are mutually cis and lie below the plane formed by the dmpe chelate rings and trans to the aryloxide ligand (Figure 6). The small angle of 66.7 (2)° between the two carbonyl groups in compounds related to **4b** has been shown to have important chemical consequences. Hence, Lippard et al. have demonstrated facile intramolecular coupling of the carbonyl groups in $TaCl(CO)_2(dmpe)_2$ under reducing conditions.[31] The two carbonyl stretching frequencies of 1805 cm^{-1} and 1740 cm^{-1} in the infrared spectrum of **4b** are very close to those (1810 cm^{-1} and 1740 cm^{-1}) reported for the chloro analogue $NbCl(CO)_2(dmpe)_2$.[32]

The electrochemistry of **4b** proves to be similar to that reported by Wreford et al. for other $XM(CO)_2(dmpe)_2$ molecules.[6] Hence a very accessible, one-electron oxidation wave at −0.31 V appears by itself to be reversible. However, it is followed very closely by a second, irreversible oxidation at +0.13 V. Hence, it appears that the initially produced 17-electron monocation $[Nb(OAr\text{-}3,5Me_2)(CO)_2(dmpe)_2]^+$ is reasonably stable for short time periods, but that further oxidation causes rapid decomposition.

The compounds obtained in this study allow some structural assessment of the variation of niobium aryloxide bonding with the formal oxidation state of the metal. In Table IX are collected together the Nb–O distances and Nb–O–Ar angles coupled with the electron configuration about the metal atom. The structural effects of oxygen-p to metal-d π-bonding in the high-valent, electron-deficient compounds can be clearly seen. If one assumes that no π-donation from the aryloxide ligand in the 18-electron carbonyl $Nb(OAr\text{-}3,5Me_2)(CO)(dmpe)_2$ (**4b**) is taking place, then a contraction from 2.181 (4) Å in this compound to as little as 1.90 (av) Å in $Nb(OAr\text{-}2,6Me_2)_5$ (**1c**) is observed. This shortening of the bond by 0.28 Å (or 13%) is comparable to the difference in bond lengths between tantalum alkyl ($Ta\text{–}CR_3$) and alkylidene ($Ta{=}CR_2$) functionalities.[33] It can be seen that the variation of the Nb–P distances for the same set of compounds is much smaller, all lying within the 2.54–2.66 Å range (Tables IV, VI, and VIII). Furthermore, it can also be seen that the correlation between electron configuration and Nb–O–Ar angles is poor. Hence, this parameter is a much less useful tool in evaluating metal-oxygen interactions of this type.

Experimental Section

General experimental procedures have been described previously.[22] The aryloxide substrates $Nb_2(OAr\text{-}4Me)_{10}$ (**1a**), $Nb_2(OAr\text{-}3,5Me_2)_{10}$ (**1b**), and $Nb(OAr\text{-}2,6Me_2)_5$ (**1c**) were prepared by literature methods.[23] Crystals of **1c** suitable for crystallographic study were obtained by slow cooling of a hot hexane solution. ^1H and ^{13}C NMR spectra were obtained with a Varian Associates XL-200 spectrometer, while ESR spectra were obtained with the nonaqueous cavity of a Varian E-line Century Series spectrometer.

$Nb(OAr\text{-}4Me)_2(dmpe)_2$ (2a). To a solution of $Nb_2(OAr\text{-}4Me)_{10}$ (2.8 g, 2.1 mmol) in toluene (100 mL) was added dmpe (1.92 g, 12.8 mmol) followed by a sodium amalgam containing Na metal (0.3 g, 13 mmol). The mixture was then stirred vigorously at room temperature in a drybox for 24 h. The resulting brown suspension was allowed to settle for 1 h before the solution was decanted off the mercury pool and filtered. Concentration of the purple filtrate followed by slow cooling produced the product as dark blocks: typical yield = 30%; EPR (toluene) g = 2.008; a(Nb) = 125 G (av). Anal. Calcd for $NbC_{26}H_{46}O_2P_4$: C, 51.40; H, 7.63; P, 20.39. Found: C, 50.95; H, 7.59; P. 20.20.

$Nb(OAr\text{-}3,5Me_2)_2(dmpe)_2$ (2b). An identical procedure to that above only using $Nb_2(OAr\text{-}3,5Me_2)_{10}$ (3.0 g, 2.15 mmol), dmpe (1.60 g, 10.8 mmol), and Na (0.35 g, 15 mmol) yielded **2b** as purple-brown crystals in typical yields of 35%; EPR (toluene) g = 2.127; a(Nb) = 123 G (av). Anal. Calcd for $NbC_{28}H_{50}O_2P_4$: C, 52.92; H, 7.93; P, 19.49. Found: C, 51.31; H, 51.31; P, 18.91.

$[Nb(OAr\text{-}3,5Me_2)_2(dmpe)_2]^+[Nb(OAr\text{-}3,5Me_2)_6]^-$ (3b). To a solution of $Nb(OAr\text{-}3,5Me_2)_2(dmpe)_2$ **2b** (0.2 g, 0.32 mmol) in benzene (25 mL) was added neat $HOAr\text{-}3,5Me_2$ (0.09 g, 0.7 mmol) with initial stirring. The purple solution turned light green, and microbubbles of H_2 (GC analysis) were formed. After 5 h crystals of the product began to slowly form and were isolated after 15 h: yield = 58%; ^1H NMR (C_6D_6, 30 °C) δ 2.16 (s, $Nb(OAr\text{-}3,5Me_2)_6^-$), 1.98 (s, $OAr\text{-}2,6Me_2$ of cation), 1.60 (m, $Me_2PCH_2PMe_2$), 1.03 (m, PCH_3). Anal. Calcd for $Nb_2C_{76}H_{95}O_8P_4$: C, 63.11; H, 6.62; P, 8.56. Found: C, 62.51; H, 6.41; P, 9.02.

$Nb(OAr\text{-}3,5Me_2)(dmpe)_2(CO)_2$ (4b). To a mixture of $Nb_2(OAr\text{-}3,5Me_2)_{10}$ (2.0 g, 1.4 mmol) and dmpe (1.1 g, 7.2 mmol) in toluene (75 mL) under an atmosphere of CO was added sodium amalgam containing 0.29 g (13 mmol) of Na metal. The mixture was stirred vigorously for 24 h. The resulting orange suspension was allowed to settle before being decanted off of the mercury pool and filtered. Concentration of the toluene filtrate and slow cooling gave the product as well-formed, air-stable orange crystals: yield = 70%; ^1H NMR (C_6D_6, 30 °C) δ 2.25 (s, $OAr\text{-}3,5Me_2$), 1.11 (m, $Me_2PCH_2PMe_2$), 1.27 (m, PCH_3); IR (Nujol mull) $\bar{\nu}$ (CO) 1805, 1740 cm^{-1}. Anal. Calcd for $NbC_{22}H_{41}O_3P_4$: C, 46.33; H, 7.25; P, 21.72. Found: C, 46.41; H, 17.31; P, 21.22.

Crystallographic Studies. One of the X-ray diffraction studies (**1c**) was completed "in-house" at Purdue University, while the other three were obtained from the Molecular Structure Center at Indiana University. General operating procedures for both units have been reviewed.[22,34] Pertinent crystallographic data is collected in Table X.

$Nb(OAr\text{-}2,6Me_2)_5$ (1c). The crystals were examined under dry, deoxygenated Nujol and mounted in an appropriately sized capillary with epoxy resin. A unique set of X-ray diffraction data were collected at low temperature on an Enraf-Nonius CAD-4 diffractometer using graphite-monochromated Mo radiation. Lattice constants were determined from a least-squares fit of 24 intensity maxima measured at $\pm 2\theta$. The structure was solved by MULTAN and refined by block-diagonal least-squares methods. The function minimized was $\sum w|F_o - F_c|^2$ with $w = 1/\sigma^2(F)$. All programs were from the SDP program library. Hydrogen atoms were located and refined isotropically. An empirical absorption connection was applied.

$Nb(OAr\text{-}4Me)_2(dmpe)_2$ (2a). A small, well-formed crystal was selected and transferred to the goniostat where it was cooled to −158 °C before characterization and data collection. A systematic search of a limited hemisphere of reciprocal space yielded a set of diffraction max-

---

(31) Bianconi, P. A.; Williams, I. D.; Engeler, M. D.; Lippard, S. J. *J. Am. Chem. Soc.* **1986**, *108*, 311.

(32) Burt, R. J.; Leigh, G. J.; Hughes, D. L. *J. Chem. Soc., Dalton Trans.* **1981**, 793.

(33) Schrock, R. R. In *Reactions of Coordinated Ligands*; Braterman, P. S., Ed.; Plenum Press: New York, 1986.

(34) Huffman, J. C.; Lewis, L. N.; Caulton, K. G. *Inorg. Chem.* **1980**, *19*, 2755.

Table X. Crystallographic Data

	1c	**2a**	**3b**	**4b**
formula	$NbC_{40}H_{45}O_5$	$NbC_{26}H_{46}O_2P_4$	$[NbC_{48}H_{45}O_6][NbC_{28}H_{50}O_2P_4]$	$NbC_{22}H_{41}O_3P_4$
fw	698.70	607.45	1455.36	570.37
space group	$P2_1/n$	$p\bar{1}$	$P2_1/a$	*Pcab*
a, Å	11.854 (4)	12.646 (4)	27.967 (23)	16.751 (3)
b, Å	16.305 (4)	14.016 (5)	23.496 (17)	12.133 (2)
c, Å	18.140 (5)	9.707 (3)	13.319 (9)	27.331 (7)
α, (deg)	90	110.87 (2)	90	90
β, (deg)	99.44 (3)	105.83 (2)	119.72 (3)	90
γ, (deg)	90	76.21 (2)	90	90
Z	4	2	4	8
V, Å^3		1527.38	7600.92	5554.68
density (calcd), g/cm^3	1.312	1.321	1.272	1.364
crystal size, mm	0.38 × 0.38 × 0.45	0.15 × 0.18 × 0.24	0.23 × 0.20 × 0.20	0.08 × 0.08 × 0.11
crystal color	yellow	purple	green	orange
radiation	Mo Kα (λ = 0.71073 Å)	Mo Kα (λ = 0.71073 Å)	Mo Kα (λ = 0.71073 Å)	Mo Kα (λ = 0.71073 Å)
linear abs coeff, cm^{-1}	3.73	6.03	4.195	6.606
temp deg °C	−115	−158	−156	−160
detector aperature	(1.5 + tan θ) mm × 4 mm high	3 mm wide × 4 mm high	3 mm wide × 4 mm high	3 mm wide × 4 mm high
takeoff angle, deg	4.9	2.0	2.0	2.0
scan speed, deg/min	variable	4.0	4.0	6.0
scan width, deg	0.8 + 0.35 tan θ	1.8 + dispersion	2.0 + dispersion	1.5 dispersion
bkgdcounts, s	50% of scan time	8	6	5
2θ range, deg	4–50	6–45	6–45	6–45
unique data	6088	4017	9914	3633
unique data with $F_o > 3.00\sigma(F)$	5033	3477	3410	2742
$R(F)$	0.036	0.0403	0.0754	0.0433
$R_w(F)$	0.045	0.0424	0.0750	0.0434
goodness of fit	1.65	1.021	1.206	0.905
largest Δ/σ	0.03	0.05	0.05	0.05

ima, which exhibited no symmetry or systematic extinctions, indicating a triclinic unit cell. The choice of the centrosymmetric space group $P\bar{1}$ was confirmed by the successful solution and refinement of the structure.

The solution of the structure was complicated by the fact that the Nb atoms were in special positions. The calculated density assuming two molecules in the unit cell was reasonable. The direct methods program MULTAN failed to locate the Nb atom. A Patterson function showed a large peak at 0.5, 0.5, 0.5. This fact combined with the intensity statistics which showed that the average intensities were large for $h + k + l = 2n$ and small for $h + k + l = 2n + 1$ led us to the conclusion that the asymmetric unit contained two Nb atoms in the special positions: 0,0,0 and 0.5, 0.5, 0.5. A difference Fourier phased on the Nb atoms showed a superposition of the two slightly different molecules. After closer inspection two sets of P and O atoms were selected, and the solution of the structure proceeded normally.

The structure was refined by full-matrix least squares, and all the hydrogen atoms were located in a difference Fourier and refined with isotropic thermal parameters, while all other atoms were refined using anisotropic thermal parameters. The final difference Fourier was essentially featureless. The unit cell contains two slightly different molecules, A and B; each possesses a crystallographic center of symmetry.

[Nb(OAr-3,5Me$_2$)$_2$(dmpe)$_2$]$^+$[Nb(OAr-3,5Me$_2$)$_6$]$^-$ (3b). A suitable sample was cleaved from a larger crystal and transferred to the goniostat where it was cooled to −156 °C for characterization and data collection. A systematic search of a limited hemisphere of reciprocal space revealed a set of diffraction maxima which could be indexed as monoclinic, space group $P2_1/a$. Subsequent solution and refinement confirmed the choice.

The structure was solved by a combination of direct methods (MULTAN78) and Fourier techniques and refined by blocked full-matrix least squares. Because of the low percentage of observed data (based on 3.00σ), no attempt was made to locate any hydrogen atoms, and only the two metals and their immediate coordination spheres were refined anisotropically. A final differences Fourier was featureless, the largest peak being 0.77 e/Å^3.

Nb(OAr-3,5Me$_2$)(CO)$_2$(dmpe)$_2$ (4b). A small, well-formed bright orange crystal was selected and transferred to the goniostat, where it was cooled to −162 °C and characterized. It was noticed that the crystal was thermochromic, and at the low temperature the color changed to clear yellow. A systematic search of a limited hemisphere of reciprocal space yielded a set of reflections which exhibited orthorhombic symmetry and systematic extinctions corresponding to the orthorhombic space group *Pcab*. This choice was confirmed by the subsequent solution and refinement of the structure.

The structure was solved by a combination of direct methods (MULTAN) and Fourier techniques. All hydrogen atoms were located in a difference Fourier computed after initial refinement of the structure. The full-matrix least-squares refinement was completed with use of anisotropic thermal parameters on all non-hydrogen atoms, while the hydrogen atoms were varied with use of isotropic *B*'s. The final difference map was essentially featureless; the maximum peak was 0.66 e/Å^3.

Acknowledgment. We thank the National Science Foundation (Grant CHE-8612063 to I.P.R.) for financial support of this work as well as for support of the Crystallographic Center at Purdue.

Registry No. 1a, 101488-19-1; **1b**, 101488-18-0; **1c**, 82182-26-1; **2a**, 101482-28-4; **2b**, 101461-80-7; **3b**, 101504-53-4; **4b**, 101461-81-8.

Supplementary Material Available: Tables of anisotropic thermal parameters and complete bond distances and angles (28 pages); listings of observed and calculated structure factors (90 pages). Ordering information is given on any current masthead page.